

Coordinated Scheduling for Interdependent Electric Power and Natural Gas Infrastructures

Anatoly Zlotnik, *Member, IEEE*, Line Roald, *Member, IEEE*, Scott Backhaus, Michael Chertkov, *Fellow, IEEE*, and Göran Andersson, *Fellow, IEEE*

Abstract—The extensive installation of gas-fired power plants in many parts of the world has led electric systems to depend heavily on reliable gas supplies. The use of gas-fired generators for peak load and reserve provision causes high intraday variability in withdrawals from high-pressure gas transmission systems. Such variability can lead to gas price fluctuations and supply disruptions that affect electric generator dispatch, electricity prices, and threaten the security of power systems and gas pipelines. These infrastructures function on vastly different spatio-temporal scales, which prevents current practices for separate operations and market clearing from being coordinated. In this paper, we apply new techniques for control of dynamic gas flows on pipeline networks to examine day-ahead scheduling of electric generator dispatch and gas compressor operation for different levels of integration, spanning from separate forecasting, and simulation to combined optimal control. We formulate multiple coordination scenarios and develop tractable physically accurate computational implementations. These scenarios are compared using an integrated model of test networks for power and gas systems with 24 nodes and 24 pipes, respectively, which are coupled through gas-fired generators. The analysis quantifies the economic efficiency and security benefits of gas–electric coordination and dynamic gas system operation.

Index Terms—Natural gas, power generation scheduling, power system security, optimal control.

I. INTRODUCTION

THE availability and low price of natural gas in North America has led to its increased use for electricity generation, which facilitated the retirement of older coal and nuclear power plants and integration of renewable resources [1]. The expansion in gas-fired generators to over 40% of installed capacity in the U.S. has brought environmental and efficiency benefits, but also created a dependence on gas concurrently with vulnerabilities in the natural gas supply chain [2]. Fuel usage of gas generators is determined by production schedules created in day-ahead electricity markets, which are cleared by balanc-

ing authorities such as independent (electric) system operators (ISOs) by solving optimization problems such as unit commitment (UC), reserve adequacy allocation, and optimal power flow (OPF) dispatch [3]–[5]. Single cycle plants can quickly go online and modulate output, and are used as marginal resources that start and shut down multiple times a day. The resulting withdrawals from gas transmission systems are highly variable and partly unpredictable because they depend on dispatch decisions in the intra-day market or as a reaction to fluctuations in generation from renewable energy sources [6], [7].

The gas transmission system historically supplied local distribution companies that buy long-term, firm contracts and withdraw gas with little intra-day variation [8]. In contrast, gas-fired power plants withdraw gas with high intra-day variability and typically purchase gas on short-term, interruptible contracts. When the gas system nears capacity and supply interruptions occur as a result, ISOs must replace production from gas-fired power plants with more expensive generation resources in intra-day operations, which challenges their ability to meet demand, maintain operating reserves, and ensure power system reliability. Conversely, gas-fired generators play a complex role in natural gas markets because their demand is price sensitive. These growing interactions present challenges that require novel and creative solutions involving inter-sector coordination [7], [9], [10].

Despite growing concerns about the lack of gas and power system coordination [11], [12], and regulatory action to reduce legal barriers in the U.S., the path to adapt market timing, regulation, and physical operations remains uncertain [13]. Infrastructure constraints can be alleviated with expansion of pipeline capacity, liquefied natural gas imports, storage for peak-shaving, dual-fueled generation, and more inter-regional electric transmission [11]. Demand-side management, more frequent gas nominations, and concurrent market clearing have also been suggested [8], [14]. However, current practices for physical system operations are not flexible enough to react to generator requirements and lack coordination across systems and regions [15]. Historical load and price analysis indicates that the Northeast U.S. experienced gas supply stress, observed as spot market basis spikes, when load levels approached 75% of firm contract capacity [11], which is conventionally identified as the constraint capacity threshold [16]. While the situation in North America motivates our investigation, the methods and analysis could be applied elsewhere. We propose that advanced control systems, information sharing, and optimization could improve the utilization of existing pipelines and interdependent power grids.

Manuscript received October 16, 2015; revised February 1, 2016; accepted March 11, 2016. Date of publication March 24, 2016; date of current version December 20, 2016. This work was supported in part under the auspices of the NNSA of the U.S. Department of Energy at Los Alamos National Laboratory under contract #DE-AC52-06NA25396, in part by DTRA Basic Research Project #10027-13399, the Advanced Grid Modeling Program in the U.S. Department of Energy Office of Electricity, and project UMBRELLA under the 7th Framework Program of the E.U. under Grant #282775. Paper no. TPWRS-01463-2015.

A. Zlotnik, S. Backhaus, and M. Chertkov are with Los Alamos National Laboratory, Los Alamos, NM 87545 USA (e-mail: azlotnik@lanl.gov; backhaus@lanl.gov; chertkov@lanl.gov).

L. Roald and G. Andersson are with the Power Systems Laboratory at the Department of Electrical Engineering, ETH Zurich, Zurich 8092, Switzerland (e-mail: roald@eeh.ee.ethz.ch; andersson@eeh.ee.ethz.ch).

Color versions of one or more of the figures in this paper are available online at <http://ieeexplore.ieee.org>.

Digital Object Identifier 10.1109/TPWRS.2016.2545522

The main control variables for gas pipelines are operating protocols for compressor stations, which boost flow to compensate for dissipative friction effects. They are usually set using steady-state models, modified ad-hoc in reaction to local conditions [17], and lack inter-regional coordination [15]. Optimization of steady-state gas flow has been formalized in optimal gas flow (OGF) problems [18]–[20], which determine optimal constant compressor station set-points that balance injections and withdrawals over a network while satisfying system pressure constraints. Steady-state models of the gas system based on the Weymouth equations [20] have been applied in previous studies on integrated gas and electricity infrastructure, such as integrated natural gas and electric OPF [21]–[23], optimal UC with natural gas security constraints [24]–[26] or to techniques for short-term operation [27], [28]. Studies on multi time-period scheduling of gas and electricity also used steady-state models [29] or coarse approximations [30], [31]. However, due to the increased influence of variable withdrawals from gas-fired generators, the steady-state assumption is no longer adequate for intra-day conditions. A feasible steady-state OGF solution may not reflect actual feasibility in real-time operation, as we subsequently show. An extension of the OGF to variable and unpredictable gas withdrawals is thus necessary to ensure secure operations, but requires dynamic modeling and optimal control strategies. This will enable pipeline operators to anticipate fluctuations in withdrawals and pressure, and prevent them from cascading throughout the system [1], [7].

Gas pipeline network dynamics are, however, notoriously difficult to simulate and optimize in a tractable way. The partial differential equations (PDEs) for gas flows comprise constraints that must be satisfied over widely distributed space and time domains with complex boundary conditions on networks, and their nonlinearity makes computational tractability a challenge [32], [33]. Recently, modeling and optimal control frameworks that closely represent the physics of gas pipelines [34] and networks [35] were developed, and were applied to solve the dynamic OGF (DOGF) with time-varying gas compression and boundary conditions. The PDE constraints were approximated by a new control system model called the reduced network flow (RNF), which was validated using traditional numerical PDE methods [34]. By applying pseudospectral discretization to the resulting optimization problem, it is possible to efficiently solve the DOGF using solvers designed for large-scale problems with sparse constraints [36]. In this paper, we couple the previously developed DOGF for the gas system with an OPF for the electric system, to obtain a method for integrated scheduling of the gas and electric systems. By utilizing the physically realistic, validated dynamic gas flow models [35], we are able to capture the effect of intra-day variability in the gas system and ensure a solution which is feasible for both sectors.

Several contributions are made here specifically to examine interdependence of power and gas system caused by intra-day interactions. First, we develop a simplified, continuous time OPF formulation, which approximates the real-time gas withdrawals of the gas-fired power plants and allows for integration with the DOGF. The integrated problem optimizes both power and gas flows to ensure a solution that is optimal and feasi-

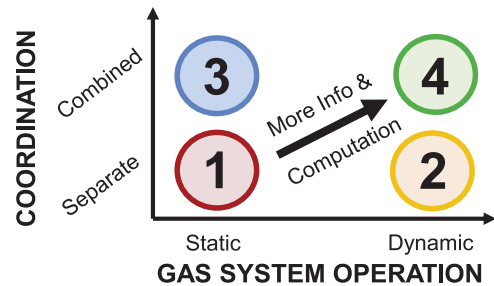


Fig. 1. Scenarios for coordination and operation of interdependent electric and gas systems.

ble for both systems, while accounting for the impact of the time-variable gas withdrawals. Second, because full coordination and co-optimization of the gas and power system would require significant regulatory and technical change, we present four operational scenarios that could be implemented as the regulatory and industry environment develops. These scenarios represent different levels of coordination (awareness and cooperation) and of capability for gas compressor operation (constant or dynamic compressor ratios), and are formalized as optimization problems. Third, we present methods to compute solutions for the scenarios, and compare them in terms of cost and feasibility under different system stress levels for coupled gas and electricity test networks. We then use an accurate simulation of the pipeline system to validate the gas pressure variations seen in the optimization solution.

Through the quantitative comparison of different operational scenarios, our approach can provide guidance to regulators and operators of gas and power systems on the economic and security benefits of various improvements to current operations. Most importantly, we observe that optimizing intra-day interactions using steady-state equations leads to pressure constraint violations, despite feasibility of the OGF itself. This suggests that physically realistic, dynamic gas flow models are necessary, despite their higher computational complexity.

The manuscript is organized as follows. In Section II, we describe the coordination and optimization scenarios to be examined. In Section III, we describe how a power production schedule estimate is obtained by solving a continuous-time OPF problem. Section IV reviews a control system model for the dynamics on gas pipeline networks. In Section V, we formulate optimization problems that are solved in each of the scenarios, and Section VI provides details related to computation. Section VII describes the test system, and is followed by the computational results and analysis in Section VIII. We summarize the implications in Section IX.

II. GAS-GRID INTEGRATION SCENARIOS

Depending on how gas pipeline industry technology, government regulations, and mechanisms for inter-sector communication evolve, several scenarios for day-ahead scheduling of interdependent power and gas systems could arise. We formulate and investigate improvements in two directions from scenario #1, which approximates the status quo, as illustrated in Fig. 1.

On the horizontal axis we consider advancement of compressor station operation from constant set-points assuming steady-state withdrawals, to model-based dynamic control that compensates for variable withdrawals. Advancement on the vertical axis represents increased coordination between the two sectors from separate optimization to full cooperation. The scenarios are described in detail below.

Scenario #1—Separate, Steady-State Power and Gas Operation: Power system operation is optimized without consideration of its effects on the gas system. The gas-fired generators contract their total gas requirements from the gas pipeline operator, who assumes that the gas is withdrawn at a constant rate and calculates constant compression set-points. This scenario represents the current operational paradigm.

Scenario #2—Dynamic Gas System Operation: As in scenario #1, power system operation ignores impacts on the gas system. However, the gas-fired generators submit their time-varying fuel burn schedules to the pipeline operator. The latter computes optimal dynamic compression protocols, which anticipate gas usage variability and the impact on pressure. The required information exchange for this scenario is possible given current regulations [37], but would require technical developments within the gas industry.

Scenario #3—Gas-Aware Power System Operation: The power system operator mitigates congestion in the gas system by adjusting gas-fired power plant fuel usage to conform with gas system limitations, assuming constant compression set-points. This scenario does not require technical changes to gas system operation, but ISOs would need gas system models and data, which requires significant regulatory changes.

Scenario #4—Integrated, Dynamic Power and Gas Operation: The operators of power and gas systems cooperate to optimize generation dispatch and time-varying gas compression to minimize overall costs. This represents the best social welfare outcome for consumers and producers in both sectors. However, it requires an entity to observe and command both systems, which is outside the current regulatory framework.

A major goal of this paper is to evaluate the performance of the interdependent systems under each of the four scenarios, and to show how undesirable operational and market outcomes can be avoided through improved control and coordination. We demonstrate the computational capability to tractably optimize operations in each scenario, and provide a dynamic gas network simulation for validating optimization results.

III. CONTINUOUS-TIME APPROXIMATION OF POWER SYSTEM SCHEDULING

In this section, we describe a simplified OPF formulation, which is used to represent power system operation and determine the day-ahead production schedule of gas-fired generators. ISOs such as PJM [4] or ISO-New England [5] clear the market by solving UC and OPF problems [3] to obtain hourly generation schedules for the following day. Intra-hour fluctuations in electricity consumption are compensated by real-time market-based rescheduling and reserve deployment. Gas-fired generators usually participate in these intra-day adjustments because of their

flexibility in changing their production, thus marginally changing gas takes relative to the day-ahead schedule. To create a day-ahead forecast of the resulting time-varying gas takes, we solve an OPF where demand and production profiles are continuous functions of time. The resulting power production profiles are translated into fuel consumption using a quadratic heat rate curve. Crucially, a continuous-time model of generator dispatch response to intra-day load variation enables mathematical integration with the smooth dynamic gas flow model in Section IV. We note that continuous-time UC formulations have been proposed as a more accurate way of handling ramping constraints [38], and do not require integer variables.

Because gas withdrawals are determined by active power generation, we model power flows in the electric system using the dc approximation, which is in agreement with previous integration studies [24], [25], [30], [31], [39]. To focus on interactions between gas and electric systems, we disregard power system constraints related to line outages, generator failures or generation ramping. Such constraints, as well as an extension to the ac power flow equations, could be included without changing the overall optimization framework, but at the cost of a more computationally complex OPF problem. The computational effort needed to solve the gas system problem would however not be affected. In combined optimization, the current OPF model balances loads and generation while ensuring gas system feasibility by changing the dispatch schedule. The integration of UC remains for future work, because combining integer variables with nonlinear, non-convex continuous equality constraints, such as for dynamic gas flow, remains a challenge in the field of optimization.

We formulate the continuous-time dc OPF as an extension to the standard single time-step formulation [40]. Let $\mathbb{G}_P = (\mathcal{V}_P, \mathcal{E}_P)$ represent the graph of the power network, where \mathcal{V}_P is the set of nodes with $|\mathcal{V}_P| = m$ and \mathcal{E}_P is the set of edges/lines of the system with $|\mathcal{E}_P| = n$. The set of generators is denoted by \mathcal{G} . To simplify notation, we assume that there is one generator with production profile $p_i(t)$ and one demand with consumption profile $h_i(t)$ per node, such that $|\mathcal{G}| = |\mathcal{V}_P| = m$. The demands $h_i(t)$ are given as continuous demand functions defined for $0 \leq t \leq T$ where $T = 24$ h. The power flows from bus i to bus j are denoted by f_{ij} , with maximum values of \bar{f}_{ij} . The objective is to minimize the total cost of generation over the time horizon $[0, T]$ where $c_i(p_i(t))$ are cost functions for production. This takes the form

$$J_P \triangleq \sum_{i \in \mathcal{G}} \int_0^T c_i(p_i(t)) dt. \quad (1)$$

The constraints for total system power balance, generator production limits, and power flow limits at all times are

$$\sum_{i \in \mathcal{V}} (p_i(t) - h_i(t)) = 0 \quad \forall t \in [0, T] \quad (2)$$

$$0 \leq p_i(t) \leq p_i^{max} \quad \forall i \in \mathcal{G} \quad \forall t \in [0, T] \quad (3)$$

$$-\bar{f}_{ij} \leq \mathbf{M}_{(ij, \cdot)}(p(t) - h(t)) \leq \bar{f}_{ij} \quad \forall \{ij\} \in \mathcal{E}_P \quad \forall t \in [0, T] \quad (4)$$

where $p(t)$ and $h(t)$ are vector functions containing $p_i(t)$ and $h_i(t)$, respectively. The matrix $\mathbf{M} \in \mathbb{R}^{n \times m}$ relates the line flows to the nodal power injections, and is defined as

$$\mathbf{M} = B_f \begin{bmatrix} (\tilde{B}_{bus})^{-1} \mathbf{0}_{m-1 \times 1} \\ \mathbf{0}_{1 \times m-1} & 0 \end{bmatrix} \quad (5)$$

where $B_f \in \mathbb{R}^{n \times m}$ is the line susceptance matrix and $\tilde{B}_{bus} \in \mathbb{R}^{m-1 \times m-1}$ is the bus susceptance matrix with the column and row corresponding to the slack bus removed [41]. $\mathbf{M}_{(ij,\cdot)}$ is the row of \mathbf{M} related to line $(i, j) \in \mathcal{E}_P$. The continuous-time dc OPF is then given by

$$\begin{aligned} \min_{p(t)} J_P \text{ in (1)} \\ \text{s.t. power system constraints: (2)–(4).} \end{aligned} \quad (6)$$

The power production profiles $p_i(t)$ for generators $i \in \mathcal{G}$ are translated into burn schedules that give gas withdrawals from the gas pipeline network using the quadratic heat rate curve

$$q(p_i) = q_0 + q_1 p_i + q_2 p_i^2. \quad (7)$$

The cost of generation is $c_i(p_i(t)) = c_g \cdot q(p_i)$ where c_g is gas price. In the following section, we describe how the effects of these withdrawals on the gas pipeline network are modeled.

IV. MODELING OF GAS NETWORK DYNAMICS

We employ a reduced control system model [35] for gas flow networks actuated by nodal compressors [35]. A network is represented as a directed graph $\mathbb{G} = (\mathcal{V}, \mathcal{E})$, where each pipe is an edge $\{i, j\} \in \mathcal{E}$ that connects nodes $i, j \in \mathcal{V}$. The instantaneous state on the edge $\{i, j\}$ is given by the density ρ_{ij} and flux φ_{ij} defined on a time interval $[0, T]$ and distance $x_{ij} \in [0, L_{ij}] = \mathcal{L}_{ij}$, where L_{ij} is the length of edge $\{i, j\}$. Assuming slow transients that do not excite shocks or waves [42], flow of gas in pipes is described by the PDEs

$$\partial_t \rho_{ij} + \partial_x \varphi_{ij} = 0 \quad \forall \{i, j\} \in \mathcal{E} \quad (8)$$

$$\partial_t \varphi_{ij} + \partial_x \rho_{ij} = -\frac{\lambda_{ij} \ell}{2D_{ij}} \frac{\varphi_{ij} |\varphi_{ij}|}{\rho_{ij}} \quad \forall \{i, j\} \in \mathcal{E}. \quad (9)$$

The parameters are the friction factor λ , pipe diameter D , speed of sound a , and length nondimensionalization ℓ . The term on the right hand side of (9) aggregates friction effects. We assume that gas pressure p and density ρ satisfy $p = a^2 \rho$ with $a^2 = ZRT$, where Z , R , and T , are the gas compressibility factor, ideal gas constant, and constant temperature.

We model gas compressor action as conservation of flow and multiplicative change in density at $x = c$, i.e., $\varphi(t, c^+) = \varphi(t, c^-)$ and $\rho(t, c^+) = \alpha(t) \rho(t, c^-)$, where $\alpha(t)$ is a compression ratio. We denote $f(c^-) = \lim_{x \nearrow c} f(x)$ and $f(c^+) = \lim_{x \searrow c} f(x)$. The required power is proportional to

$$C \propto \eta^{-1} |\varphi(t, c)| (\max\{\alpha(t), 1\}^{2m} - 1) \quad (10)$$

with $0 < m < (\gamma - 1)/\gamma < 1$ where γ is the heat capacity ratio and η is the compressor efficiency [18], [19]. We define the set of controllers $\mathcal{C} \subset \mathcal{E} \times \{+, -\}$, where $\{i, j\} \equiv \{i, j, +\} \in \mathcal{C}$ (resp. $\{j, i\} \equiv \{i, j, -\}$) denotes a controller located at node $i \in \mathcal{V}$ (resp. j) that augments the density of gas flowing into

edge $\{i, j\} \in \mathcal{E}$ in the $+$ (resp. $-$) direction. Compression is modeled as a ratio $\alpha_{ij} : [0, T] \rightarrow \mathbb{R}_+$ for $\{i, j\} \in \mathcal{C}$.

We denote by $s_j : [0, T] \rightarrow \mathbb{R}$ the density of gas entering the network from a node $j \in \mathcal{V}_S$, where \mathcal{V}_S is the set of supply terminals called ‘‘slack’’ junctions, able to supply any mass flux at the given density. A mass flux withdrawal (or injection, if negative) at a junction $j \in \mathcal{V}_D = \mathcal{V} \setminus \mathcal{V}_S$ is denoted by $d_j : [0, T] \rightarrow \mathbb{R}$, where \mathcal{V}_D is the set of demand (non-‘‘slack’’) nodes. The functions $\{\alpha_{ij}\}_{\{i,j\} \in \mathcal{C}}$, $\{d_j\}_{j \in \mathcal{V}_D}$, and $\{s_j\}_{j \in \mathcal{V}_S}$ create nodal balance conditions of the form

$$\begin{aligned} \alpha_{ji}(t) \rho_{jk}(t, 0) &= \alpha_{jk}(t) \rho_{ij}(t, L_j) \\ \forall j \in \mathcal{V}_D \text{ and } \{i, j\}, \{j, k\} \in \mathcal{E}, \end{aligned} \quad (11)$$

$$d_j(t) = \sum_{i \in \mathcal{V}_D} \varphi_{ij}(t, L_{ij}) - \sum_{k \in \mathcal{V}_D} \varphi_{jk}(t, 0) \quad \forall j \in \mathcal{V}_D, \quad (12)$$

$$\rho_{ij}(t, 0) = s_i(t) \quad \forall i \in \mathcal{V}_S. \quad (13)$$

We use a reduced control system model for the network flow dynamics (8), (9) with nodal conditions (11)–(13). Suppose that $V = |\mathcal{V}_D|$ and $E = |\mathcal{E}|$, and assign to each edge an index in $[E]$, where $[N] = (1, \dots, N)$ for a positive integer $N \in \mathbb{N}$, using the mapping $\pi_e : \mathcal{E} \rightarrow [E]$. Each node in \mathcal{V}_D is assigned a unique internal density and each edge in \mathcal{E} is assigned a flow, yielding the nodal density and edge flow state vectors $\rho = (\rho_1, \dots, \rho_V)^T$ and $\varphi = (\varphi_1, \dots, \varphi_E)^T$. We define the collection of nodal withdrawal fluxes $d = (d_1, \dots, d_V)^T$, where d_k is negative if an injection. Also define the slack node densities as $s = (s_1, \dots, s_b)^T$, where $b = |\mathcal{V}_S|$. Define the diagonal matrices $\Lambda, K \in \mathbb{R}^{E \times E}$ by $\Lambda_{kk} = L_k$ and $K_{kk} = \ell \lambda_k / D_k$, where L_k, λ_k , and D_k are the nondimensional length, friction coefficient, and diameter of edge $k = \pi_e(ij)$.

We then define the time-dependent weighted incidence matrix $B : \mathbb{R}^E \rightarrow \mathbb{R}^{|\mathcal{V}|}$ by

$$B_{ik} = \begin{cases} \alpha_{ij}, & \text{edge } k = \pi_e(ij) \text{ enters node } i, \\ -\alpha_{ij}, & \text{edge } k = \pi_e(ij) \text{ leaves node } i, \\ 0, & \text{else} \end{cases} \quad (14)$$

as well as the incidence matrix $A = \text{sign}(B)$. Let $A_s, B_s \in \mathbb{R}^{b \times E}$ denote submatrices of rows of A and B corresponding to \mathcal{V}_S , and let $A_d, B_d \in \mathbb{R}^{V \times E}$ correspond similarly to \mathcal{V}_D . Define the function $g : \mathbb{R}^E \times \mathbb{R}_+^E \rightarrow \mathbb{R}^E$ by $g_j(x, y) = x_j |x_j| / y_j$. The RNF ODE model is given by

$$\dot{\rho} = (|A_d| \Lambda |B_d^T|)^{-1} [4(A_d \varphi - d) - |A_d| \Lambda |B_s^T| \dot{s}], \quad (15)$$

$$\dot{\varphi} = -\Lambda^{-1} (B_s^T s + B_d^T \rho) - Kg(\varphi, |B_s^T| s + |B_d^T| \rho). \quad (16)$$

For a connected graph, $A_d \in \mathbb{R}^{V \times E}$ and $B_d \in \mathbb{R}^{V \times E}$ are full rank, and therefore $|A_d| \Lambda |B_d^T|$ is invertible. Time-varying parameters are gas withdrawals $d \in \mathbb{R}^V$, input densities $s \in \mathbb{R}_+^b$, and compressions $\alpha_{ij} \in \mathcal{C}$. The RNF (15), (16) is a consistent spatial discretization of the PDE (8), (9) [34], [35], and reduces to the static balance laws in the steady-state [19], [35].

We discretize (15), (16) in time for optimal control as part of scenarios #2 to #4, and set the left hand side of (15), (16) to zero for steady-state constraints for the OGF in scenario #1. The control variables for the gas system are compression ratios α_{ij}

for $\{i, j\} \in \mathcal{C}$, where $C = |\mathcal{C}|$ is the number of compressors. Let $\alpha = (\alpha_1, \dots, \alpha_C)'$ be a vector containing the compression ratios such that α_k is indexed by $k = \pi_c(i, j)$, where the map $\pi_c : \mathcal{C} \rightarrow [C]$ defines a re-indexing of \mathcal{C} . The equations (15) and (16) are also used for simulation of gas network transients.

V. OPTIMAL CONTROL FORMULATIONS

We first describe how gas burn schedules of gas-fired generators can be used by a gas pipeline operator to compute an OGF for scenario #1, or a DOGF for scenario #2, where the systems are optimized separately. Then, we describe the combined optimization schemes in scenarios #3 and #4.

A. Scenario #1: Best Status Quo Paradigm

First, gas-fired generator fuel burn schedules $d_i(t) = q(p_i(t))$ for $i \in \mathcal{G}$ are approximated by solving the continuous-time OPF problem (6) and then applying (7). The gas withdrawal profiles $d_j(t)$ for gas system nodes $j \in \mathcal{V}_D$ are averaged to yield steady withdrawals d_j . These are passed to the pipeline operator, who obtains constant gas compressor set-points α_{ij} by solving the steady-state OGF [19]. Errors related to steady-state modeling require a conservative estimate of necessary compression ratios, so we multiply each withdrawal d_j by a factor of 1.25 when computing the OGF. The compressor set-points are computed by minimizing the objective

$$J_G^s \triangleq \sum_{\{i,j\} \in \mathcal{C}} \frac{|\varphi_{\pi_c(ij)}|}{\eta_{ij}} ((\max\{\alpha_{ij}, 1\})^{2m} - 1), \quad (17)$$

which aggregates compression costs of the form (10) throughout the network, and where η_{ij} is the efficiency of compressor $\{i, j\} \in \mathcal{C}$. The steady-state flow physics are enforced by setting the left hand side of (15) and (16) to zero, yielding

$$d = A_d \varphi, \quad (18)$$

$$(B_s^T s + B_d^T \rho) = -\Lambda K g(\varphi, |B_s^T| s + |B_d^T| \rho). \quad (19)$$

Nodes are subject to steady withdrawals d_j for $j \in \bar{\mathcal{V}}_D$, available supply densities s_j for $j \in \mathcal{V}_S$. Box constraints on system pressure and compressor actuation given by

$$\rho_i^{\min} \leq \alpha_{ij} \rho_i \leq \rho_i^{\max} \quad \forall i \in \bar{\mathcal{V}}_D, \quad (20)$$

$$1 \leq \alpha_{ij} \leq \alpha_{ij}^{\max} \quad \forall \{i, j\} \in \mathcal{C}, \quad (21)$$

must be enforced. Thus, the steady-state OGF problem is

$$\begin{aligned} \min_{\alpha, \rho, \varphi} \quad & J_G^s \text{ in (17)} \\ \text{s.t.} \quad & \text{static RNF constraints: (18) - (19)} \\ & \text{box constraints: (20), (21).} \end{aligned} \quad (22)$$

A feasible steady-state solution of (22) does not guarantee feasibility given time-varying gas withdrawals $d_i(t)$.

B. Scenario #2: Dynamic Gas System Operation

As in scenario #1, gas power plant burn schedules $d_i(t) = q(p_i(t))$ for $i \in \mathcal{G}$ are approximated by solving the continuous-time OPF problem (6) and then applying (7). Again, only the

expected fuel usage of gas-fired power plants is exchanged between industry sectors, but now the time-dependence of the withdrawals $d_j(t)$ is included. The gas system operator then optimizes the time-varying compression ratios $\alpha(t)$ based on the dynamics (15), (16), in order to anticipate system-wide changes. We formulate the DOGF for day-ahead gas system operation over a 24-h period $[0, T]$. The edge dynamics (8), (9) and nodal conditions (11)–(13) are enforced with the RNF (15), (16). Nodes are subject to transient withdrawals $d_j(t)$ for $j \in \bar{\mathcal{V}}_D$, available supply densities $s_j(t)$ for $j \in \mathcal{V}_S$, and box constraints

$$\rho_i^{\min} \leq \alpha_{ij}(t) \rho_i(t) \leq \rho_i^{\max} \quad \forall i \in \bar{\mathcal{V}}_D \quad (23)$$

$$1 \leq \alpha_{ij}(t) \leq \alpha_{ij}^{\max} \quad \forall \{i, j\} \in \mathcal{C}, \quad (24)$$

on the density and compression. For simplicity, we choose time-periodic terminal conditions of the form

$$\rho(0) = \rho(T), \varphi(0) = \varphi(T), \quad (25)$$

$$\alpha_{ij}(0) = \alpha_{ij}(T) \quad \forall \{i, j\} \in \mathcal{C}. \quad (26)$$

The DOGF objective function, which aggregates compression costs of the form (10) throughout the network, is

$$J_G^d \triangleq \sum_{\{i,j\} \in \mathcal{C}} \int_0^T \frac{|\varphi_{\pi_c(ij)}(t)|}{\eta_{ij}} ((\max\{\alpha_{ij}(t), 1\})^{2m} - 1) dt. \quad (27)$$

We formulate the DOGF for day-ahead gas system operation over a 24-h period $[0, T]$, where decision functions are the vector of nodal compression ratios $\alpha(t)$. That is,

$$\begin{aligned} \min_{\alpha(t), \rho(t), \varphi(t)} \quad & J_G^d \text{ in (27)} \\ \text{s.t.} \quad & \text{dynamic RNF constraints: (15), (16)} \\ & \text{box constraints: (23), (24)} \\ & \text{terminal constraints: (25), (26).} \end{aligned} \quad (28)$$

If a solution to problem (28) exists, then applying the corresponding compression ratio profiles $\alpha_{ij}(t)$ guarantees feasible pressures for dynamic gas withdrawal profiles $d_i(t)$.

C. Scenario #3: Gas-Aware Power System Operation

Scenario #3 represents gas-aware power system operation, where the OPF is solved subject to dynamic gas constraints (15), (16) but with constant compression ratios α_{ij} (20), (21). The formulation is

$$\begin{aligned} \min_{p(t), \alpha, \rho(t), \varphi(t)} \quad & \beta_P J_P + \beta_G J_G^d \text{ using (1) and (27)} \\ \text{s.t.} \quad & \text{power system constraints: (2)–(4)} \\ & \text{generator heat-rate coupling: (7)} \\ & \text{dynamic RNF constraints: (15), (16)} \\ & \text{gas box constraints: (21), (23),} \\ & \text{terminal constraints: (25), (26).} \end{aligned} \quad (29)$$

The power and gas systems are coupled in problem (29) through the generator heat rate curve (7), which relates gas-fired generator fuel usage to power output. Minimization is over both the power generation $p(t)$ and the vector of constant compression

ratios α . The scaling coefficients β_P and β_G are used to appropriately weight the power and gas system objectives, respectively. Because many possible compression ratio profiles could be used to provide feasible gas withdrawals $d_j(t)$ from the gas system, we add the compression cost to the objective function to make the problem well-posed and guarantee a consistent solution. Minimizing costs for the ISO while maintaining feasible gas system pressure is the primary priority, while minimizing compressor operation costs is secondary. Therefore, we choose weights β_P and β_G to get $\beta_P J_P \approx 10^2 \beta_G J_G^d$ so the weighted compression cost is small compared to generation cost. This ensures a regular solution for α without significantly altering the power schedule.

If a feasible solution to problem (29) exists, applying the constant compression ratios α_{ij} guarantees feasibility for the gas system given the dynamic gas withdrawal profiles $d_j(t)$ corresponding to gas-fired generators. To obtain this jointly feasible solution, the power production profiles $p_i(t)$ for $i \in \mathcal{G}$ may move away from the optimum of the stand-alone power production scheduling problem (6).

D. Scenario #4: Joint Dynamic Power and Gas Optimization

Scenario #4 represents full coordination between gas and electric systems, with time-varying controls $\alpha(t)$ for the gas compressors. Both power generation $p(t)$ and compression policies $\alpha(t)$ are optimized, with scaling coefficients β_P , β_G for power and gas system objectives as in scenario #3. The formulation is

$$\begin{aligned} & \min_{p(t), \alpha(t), \rho(t), \varphi(t)} \beta_P J_P + \beta_G J_G^d \text{ using (1) and (27)} \\ \text{s.t.} & \text{ power system constraints: (2)–(4)} \\ & \text{ generator heat-rate coupling: (7)} \\ & \text{ dynamic RNF constraints: (15), (16)} \\ & \text{ gas box constraints: (23), (24)} \\ & \text{ terminal constraints: (25), (26).} \end{aligned} \quad (30)$$

If a feasible solution to problem (30) exists, then applying the corresponding compression ratio profiles $\alpha_{ij}(t)$ guarantees feasibility for the gas system given the dynamic gas withdrawal profiles $d_j(t)$ corresponding to gas-fired generators. Though power production $p_i(t)$ may move away from the optimum of the stand-alone OPF (6) to enable feasibility for the combined problem, the permission of dynamic compression ratios increases the set of feasible solutions. Thus the optimum of (30) will have lower cost than that of problem (29).

VI. COMPUTATIONAL FRAMEWORK

In this section, we describe the computational schemes used to solve the optimization problems for the four scenarios, as well as to subsequently simulate gas flow dynamics to validate and analyze the outcome. For both purposes, the discretization used in the RNF must be sufficiently fine to accurately approximate the PDE dynamics. We first create a modified graph $\overline{\mathcal{G}} = (\overline{\mathcal{V}}, \overline{\mathcal{E}})$ by adding nodes such that all edges of $\overline{\mathcal{E}}$ are shorter than a maximum length ℓ , which is used as the non-dimensional constant. It has been observed [44], and we have confirmed [34], that $\ell = 10$

km is sufficient to adequately represent transients of interest. The RNF is then defined using $\overline{\mathcal{G}}$ for optimal control and simulation.

A. Computation of Optimal Controls

The problems formulated in (6) and (28)–(30) are constrained optimization problems on continuous function spaces, which we approximate using NLPs through pseudospectral discretization using the Legendre–Gauss–Lobatto (LGL) pseudospectral collocation scheme [45]. Each state and control function is approximated by a polynomial, and the optimization decision variables are coefficients of the polynomial expansions at the LGL time-collocation points. We use 36 collocation points in time to represent these functions over the 24-h optimization period for all scenarios. The representation of continuous dynamics using polynomials gives spectral accuracy, which yields high fidelity even with coarse discretization using few decision variables. This transcription is described in the context of gas networks in our previous work [35]. The computation is implemented by using a MATLAB interface to provide functions for the objective, constraints, and their gradients with respect to the decision variables (the polynomial coefficients), to the interior-point solver IPOPT version 3.11.8 running with the linear solver ma57 [36]. The gradient functions have on the order of 1% non-zero entries, so the sparse linear algebra routine ma57 greatly speeds solution. Though the gas dynamics are in general non-convex, we observe consistent convergence to the same solutions given random initializations. Note that while problem (6) lacks dynamic constraints, so polynomial approximation is not necessary, it is solved on the same time-collocation points as the DOGF problem to enable the combined optimization implementations in scenarios #3 and #4. The steady-state NLP (22) does not require approximations for time-discretization, and is solved directly using IPOPT.

In the combined optimization problems in scenarios #3 and #4, numerical scaling of the power and gas network subproblems is a challenging computational issue. The Jacobian of the joint constraints must have good condition, i.e., without eigenvalues on very different scales, for the optimization to converge well. Therefore, the relative scaling of the problems must be adjusted without modifying the solution. The overall problem is scaled so the objective function value is on the order of 1, and absolute and relative tolerances of 10^{-4} are used in IPOPT. Once the appropriate scaling is found for specific systems under standard conditions, the same scaling can be used for subsequent computations. The interplay between problem dimension, numerical stability, and fineness of spatial discretization of the gas network also requires further study.

B. Simulation of Gas Flow Dynamics

After optimization for each scenario is concluded, the solutions are validated to verify feasibility, check for numerical errors, and confirm suitable problem scaling. The compressor ratios and initial pressure conditions are used in an explicit continuous-time simulation of (15) and (16), where a relative error tolerance of 10^{-4} is enforced. The simulation is implemented using the low-order solver `ode15s` for stiff ODE systems in

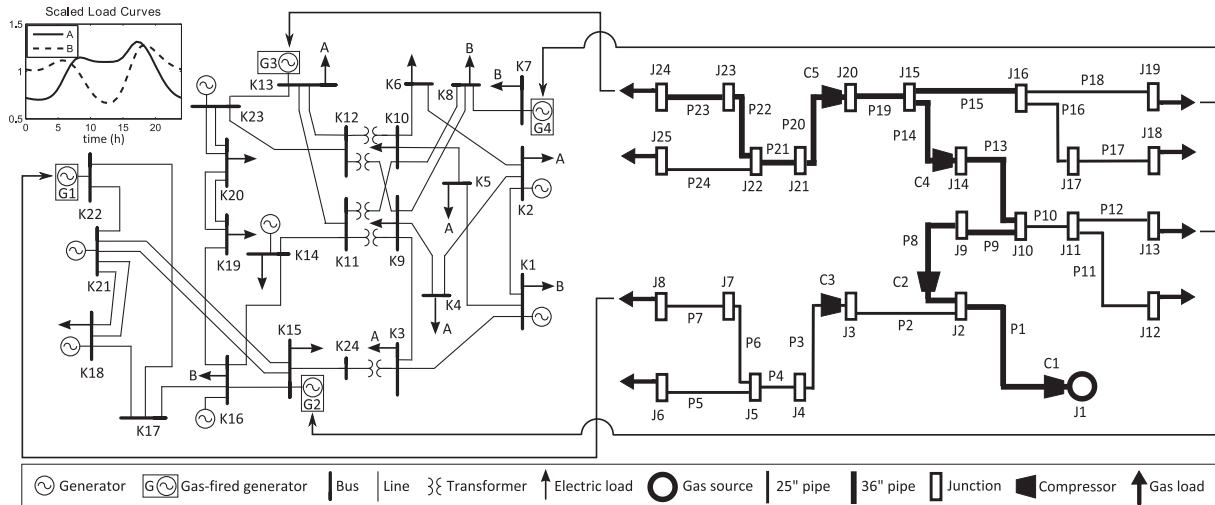


Fig. 2. Schematic of integrated electric and gas test networks (data online [43]). IEEE RTS96 One Area 24 node power system (left) coupled with the 24 pipe benchmark gas system (right) through gas-fired generators (G1 to G4). Electric loads marked with A or B are scaled by the time-varying load curves in the inset plot at top left. Electric buses (K1 to K24), gas pipes (P1 to P24), pipe junctions or network nodes (J1 to J25), and gas compressors (C1 to C5) are indicated.

MATLAB, where adaptive time-stepping is used to maintain error tolerance. The simulation has been validated in previous work [34], and has been used to evaluate optimization fidelity [46]. The simulation runs require between 1 and 10 seconds, depending on rates of change in withdrawals $d(t)$, to simulate the 24-pipe gas test network for a 24-h period.

VII. TEST SYSTEM

For the case studies we employ the 24-node IEEE One Area RTS-96 test network [47] coupled with the 24-pipe benchmark gas system test network (online [43]), as shown in Fig. 2. The production limits of generators in the power system test network are scaled such that total generation capacity is 2724 MW. The line capacities are reduced to 50%, and system loads are scaled to 80% of nominal values. Some loads are scaled according to one of two time-varying curves (A or B) inset at top left in Fig. 2. Low, baseline, and high system stress levels are defined by scaling the remaining constant electric loads to 25%, 50%, and 65% of nominal values, respectively. We place gas-fired shoulder plants at buses 7 and 13, and peak power plants at 15 and 22, for which the costs $c(p_i) = c_g q(p_i)$ of generations p_i are determined based on gas usage computed through the quadratic heat rate curve in (7). The coefficients used are $(q_0, q_1, q_2) = (3.08, 0.48, 0.001)$ for a peaking plant and $(7.83, 0.26, 0.0015)$ for a shoulder plant [48]. The flows $q(p_i)$ are translated into cost at a gas price of $c_g = 6$ \$/mmBTU. Cost coefficients for the remaining generators are taken from MatPower [49]. The generators draw fuel from the gas system test network, where the friction factor and sound speed parameters used for the gas pipelines are $\lambda = 0.01$ and $a = 377.968$ m/s. Gas-fired units at power system nodes 22, 15, 13, and 7 draw fuel from gas system nodes 8, 13, 24, and 19, respectively. The integrated model is scaled so that 40% of generating capacity is gas-fired, and approximately 50% of gas is used for power in the baseline

case. The customers at gas system nodes 6, 12, 18, and 25 each use the remaining gas at a mean rate of 40 kg/s, weighted by the A profile in the inset plot in Fig. 2. Gas is available at the “slack” node at junction 1 at 500 psi, and boosted into the system by compressor 1, with a total daily system throughput on the order of 500 000 mmBTU. Pressure and compression ratios are bounded in [500, 800] psi and [1, 2], respectively.

VIII. RESULTS AND ANALYSIS

We show results for the baseline and high system stress levels in Figs. 3 and 4, respectively, with outcomes of scenarios #1 to #4 shown in columns from left to right. In each column, the gas-fired generator production (MW) is shown at bottom, and constant or time-varying compression ratios are shown at center. Those compression ratios and gas takes corresponding to the generation profiles are then applied in a simulation of the gas pipeline system, for which the pressure trajectories throughout the network are shown at top. This simulation also serves to confirm that the solution of the discretized optimization problem actually satisfies pressure constraints placed on the continuous system.

A. Baseline Stress Level

Observe that even using a capacity margin of 25% when solving (22) leads to pressure infeasibility in the dynamic simulation for scenario #1, which is similar to observations of current operations [17]. However, the model-based control in scenario #2 yields a solution in which pressure remains within limits. For scenario #3, the power production schedule and constant gas compression ratios are computed jointly, yielding different results from those of scenario #1. By incorporating dynamic constraints for the gas system into the OPF, we regain feasible solutions for both the power and gas systems. The OPF cost in scenario #3 is higher by 5% because scheduling must change

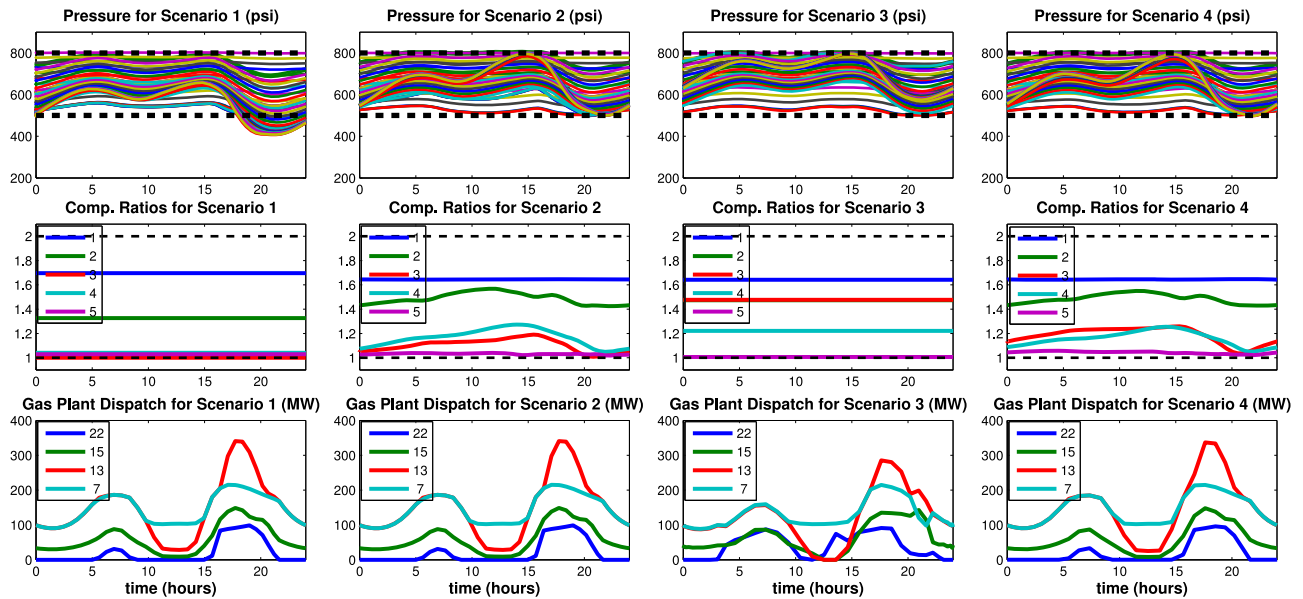


Fig. 3. Comparison of scenarios #1 (left) to #4 (right) for the baseline case. From top to bottom: Simulated nodal pressures (color) and pressure bounds (dashed); compression ratios; gas-fired generator dispatch solutions.

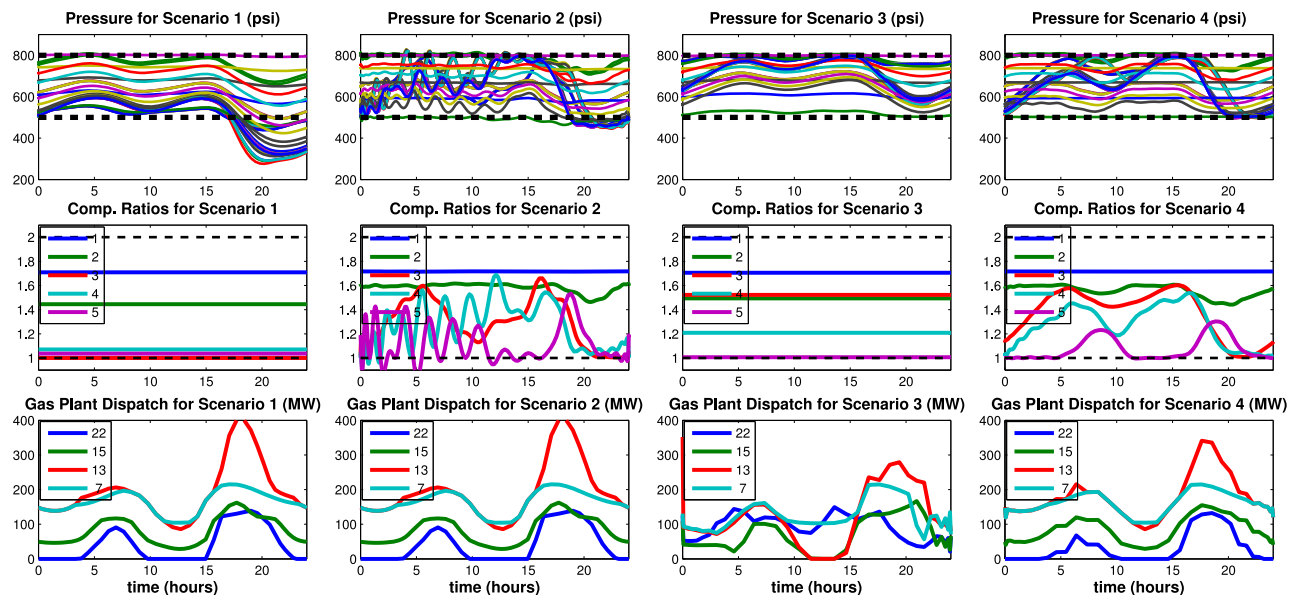


Fig. 4. Comparison of scenarios #1 (left) to #4 (right) for the high stress case. From top to bottom: Simulated nodal pressures (color) and pressure bounds (dashed); compression ratios; gas-fired generator dispatch solutions.

away from the optimum to maintain gas system feasibility. When the power production schedule and time-varying gas compression ratios are optimized jointly in scenario #4, compressor ratio profiles are very similar to those in scenario #2, and OPF cost is the same as in scenarios #1 and #2. This similarity indicates that the scheduling problems of power and gas systems are separable in the baseline case when dynamic gas system control is used.

B. High Stress Level

As in the baseline case, the compression ratios obtained with the steady-state OGF in scenario #1 result in pressure

TABLE I
COMPUTATION TIMES

Stress cases	Computation time (seconds)			
	Sc. #1	Sc. #2	Sc. #3	Sc. #4
low (25%)	13	1087	355	3160
base (50%)	14	666	938	3100
high (65%)	16	1205	1740	2388

violations in the dynamic regime. Scenario #2 (with dynamic compressor ratios) does not have a feasible solution, although the solver reaches maximum iterations with a better solution

TABLE II
COMPARISON OF METRICS FOR SCENARIOS AND STRESS CASES

Stress cases	DC OPF objective (\$ $\times 10^6$)				Pressure Violation Norm (psi-days)				Gas Usage for Generation (mmBTU $\times 10^5$)			
	<i>Sc.</i> #1	<i>Sc.</i> #2	<i>Sc.</i> #3	<i>Sc.</i> #4	<i>Sc.</i> #1	<i>Sc.</i> #2	<i>Sc.</i> #3	<i>Sc.</i> #4	<i>Sc.</i> #1	<i>Sc.</i> #2	<i>Sc.</i> #3	<i>Sc.</i> #4
low (25%)	0.5972	0.5972	0.5971	0.5971	4.5794	0.1146	0.1309	0.0843	2.1446	2.1446	2.1415	2.1414
base (50%)	0.7316	0.7316	0.7532	0.7316	83.751	0.1923	0	0.0255	3.0608	3.0608	3.0981	3.0593
high (65%)	0.8256	0.8256	1.0250	0.8883	303.61	56.925	0	1.0802	3.8015	3.8015	3.4075	3.6244

with lower pressure violations than the steady-state OGF. For systems near capacity, dynamic gas system optimization based on time-varying gas withdrawals cannot alone guarantee security in the high stress case. Therefore, increased levels of data and model coordination are required. In scenario #3, production is shifted from gas-fired generators to other more expensive resources, causing a generation cost increase of 24% over the gas-independent dispatch in scenarios #1 and #2. However, the fully integrated, transient solution in scenario #4 is not only feasible, but requires only 7% generation cost increase over scenario #1.

C. Computation Time

Sample times required to perform optimization for each scenario and stress case on a commodity computing platform (laptop with Intel i5 processor) are shown in Table I. Computation may be affected by problem scaling, because IPOPT uses relative and absolute tolerances under various circumstances. A computation time of under an hour is always achieved, which allows computing schedules for the following day. Implementation of production codes on higher performance computing platforms would significantly reduce solution time.

D. Quantifying Costs, Benefits, and Feasibility

In order to make a straightforward comparison between the coordination scenarios in the three stress cases, we compare the OPF objective function value, the total daily gas used for generation, and the L_2 norm of pressure constraint violation. The latter is of the form $v_\rho = \|V_\rho\|_2$, where

$$V_\rho = \left[\int_0^T (p(t) - p_{\max})_+^2 dt \right]^{\frac{1}{2}} + \left[\int_0^T (p_{\min} - p(t))_+^2 dt \right]^{\frac{1}{2}} \quad (31)$$

and $(x)_+ = x$ if $x \geq 0$ and $(x)_+ \equiv 0$ if $x < 0$. These metrics allow us to quantify the costs and benefits of the scenarios at various levels of system stress. Their values for the four scenarios in Section II under low, base, and high stress levels are given in Table II. The pressure violation metrics are computed by using the ODE solution of the RNF for the compression ratio solutions from the preceding optimization.

Moving from scenario #1 to #2, i.e., implementing advanced gas system control with optimal time-varying gas compression, results in much lower pressure violations. This alone goes far towards ensuring gas system security and fuel supplies to the electricity grid when both systems are stressed. Such improvement can be made within the current U.S. regulatory frame-

work, which permits communication of scheduled day-ahead gas and power flows [37]. However, it requires pipeline operators to change their day-ahead scheduling and compressor control strategies. Moving from scenario #1 to #3, i.e., implementing information sharing and combined optimization under current gas system operating practices using steady-state models, removes pressure violations but at significantly increased generation dispatch cost. This would require regulatory change and new market mechanisms, but minimal changes to compressor operation. Moving to scenario #4 eliminates pressure violations at moderately increased dispatch cost, but requires both regulatory and technological transitions.

IX. CONCLUSION

We have presented an analysis framework for dynamic scheduling and simulation of coupled electric power and natural gas infrastructures where intra-day interdependence effects are closely approximated. We formulate optimization problems for different coordination scenarios, from none to fully integrated optimization, and for different operational methods for gas compressors. In each case, numerical solutions to optimization problems with gas dynamics are validated using continuous-time simulations. This methodology enables performance assessment at various levels of coordination and operational sophistication, and quantifies the benefits of coordination between the sectors. In particular, we conclude that while dynamic gas system control and increased coordination each provide benefits, both are required for security and economic efficiency under high stress conditions. Although fully cooperative, combined optimization may not be possible in practice, it is valuable to examine the benefits that such best-case scenarios would bring. The preliminary results above still require improvement in modeling and computation, as well as confirmation through studies using extensive multi-year operational data. The significant benefits observed warrant future work that explores optimization algorithms with more comprehensive power system models, and that allow for iterative exchange of only limited information, such as feasibility cuts and/or marginal prices.

ACKNOWLEDGMENT

The authors would like to thank R. Bent, S. Blumsack, and S. Misra for valuable discussions.

REFERENCES

- [1] R. Levitan *et al.*, "Pipeline to reliability: Unraveling gas and electric interdependencies across the eastern interconnection," *IEEE Power Energy Mag.*, vol. 12, no. 6, pp. 78–88, Nov./Dec. 2014.

- [2] M. Shahidepour and Z. Li, "White paper: Long-term electric and natural gas infrastructure requirements," Illinois Inst. Technol., Chicago, IL, USA, Tech. Rep., 2014.
- [3] E. Litvinov, "Design and operation of the locational marginal price-based electricity markets," *IET Gener., Transmiss. Distrib.*, vol. 4, no. 2, pp. 315–323, Feb. 2010.
- [4] Forward Market Operations, "Energy & ancillary services market operations, M-11 Rev. 75," PJM, Tech. Rep., 2015.
- [5] ISO New England, "ISO New England manual for market operations, M-11 Rev. 49," ISONE, Tech. Rep., 2014.
- [6] P. Weigand, G. Lander, and R. Malmé, "Synchronizing natural gas & power markets: A series of proposed solutions," Skipping Stone Energy Market Consultants, Tech. Rep., 2013.
- [7] M. Chertkov, M. Fisher, S. Backhaus, R. Bent, and S. Misra, "Pressure fluctuations in natural gas networks caused by gas-electric coupling," in *Proc. IEEE 48th Hawaii Int. Conf. Syst. Sci.*, 2010, pp. 2738–2747.
- [8] R. Rubio, D. Ojeda-Esteybar, O. Ano, and A. Vargas, "Integrated natural gas and electricity market: A survey of the state of the art in operation planning and market issues," in *Proc. IEEE/PES Transmiss. Distrib. Conf. Expo., Latin Amer.*, 2008, pp. 1–8.
- [9] R. D. Tabors and S. Adamson, "Measurement of energy market inefficiencies in the coordination of natural gas & power," in *Proc. IEEE 47th Hawaii Int. Conf. Syst. Sci.*, 2014, pp. 2335–2343.
- [10] M. Chertkov, S. Backhaus, and V. Lebedev, "Cascading of fluctuations in interdependent energy infrastructures: Gas-grid coupling," *Appl. Energy*, vol. 160, pp. 541–551, 2015.
- [11] Black and Veatch, "New England natural gas infrastructure and electric generation: Constraints and solutions," The New England States Committee on Electricity, Tech. Rep., 2013.
- [12] MITEI. (2013). Growing concerns, possible solutions: The Interdependency of Natural Gas and Electricity Systems [Online]. Available: <http://mitei.mit.edu/publications/reports-studies/growing-concerns-possible-solutions>
- [13] R. D. Tabors, S. Englander, and R. Stoddard, "Who's on first? the coordination of gas and power scheduling," *Electricity J.*, vol. 25, no. 5, pp. 8–15, 2012.
- [14] P. J. Hibbard and T. Schatzki, "The interdependence of electricity and natural gas: current factors and future prospects," *Electricity J.*, vol. 25, no. 4, pp. 6–17, 2012.
- [15] S. Thumb *et al.*, "Natural gas market regionalization and implications," Electric Power Research Institute, Tech. Rep., 1998.
- [16] T. Koch *et al.*, *Evaluating Gas Network Capacities*. Philadelphia, PA, USA: SIAM, 2015.
- [17] Tennessee gas pipeline company ISO NE presentation: Mar. 24, 2011 [Online]. Available: http://iso-ne.com/committees/comm_wkgrps/othr/egoc/mtrls/2011/mar302011/el_paso_isone_necpuc_032411.pdf
- [18] P. Wong and R. Larson, "Optimization of natural-gas pipeline systems via dynamic programming," *IEEE Trans. Automat. Control*, vol. AC-13, no. 5, pp. 475–481, Oct. 1968.
- [19] S. Misra, M. W. Fisher, S. Backhaus, R. Bent, M. Chertkov, and F. Pan, "Optimal compression in natural gas networks: A geometric programming approach," *IEEE Trans. Control Netw. Syst.*, vol. 2, no. 1, pp. 47–56, Mar. 2015.
- [20] R. Z. os-RiMercado and C. Borraz-Sánchez, "Optimization problems in natural gas transportation systems: A state-of-the-art review," *Appl. Energy*, vol. 147, pp. 536–555, 2015.
- [21] S. An, Q. Li, and T. W. Gedra, "Natural gas and electricity optimal power flow," in *Proc. IEEE Transmiss. Distrib. Conf. Expo.*, 2003, vol. 1, pp. 138–143.
- [22] M. Geidl and G. Andersson, "Optimal power flow of multiple energy carriers," *IEEE Trans. Power Syst.*, vol. 22, no. 1, pp. 145–155, Feb. 2007.
- [23] C. Unsuhay *et al.*, "Modeling the integrated natural gas and electricity optimal power flow," in *Proc. IEEE Power Eng. Soc. Gen. Meet.*, 2007, pp. 1–7.
- [24] T. Li, M. Eremia, and M. Shahidepour, "Interdependency of natural gas network and power system security," *IEEE Trans. Power Syst.*, vol. 23, no. 4, pp. 1817–1824, Nov. 2008.
- [25] C. Liu, M. Shahidepour, Y. Fu, and Z. Li, "Security-constrained unit commitment with natural gas transmission constraints," *IEEE Trans. Power Syst.*, vol. 24, no. 3, pp. 1523–1536, Aug. 2009.
- [26] C. M. Correa-Posada and P. Sánchez, "Security-constrained optimal power and natural-gas flow," *IEEE Trans. Power Syst.*, vol. 29, no. 4, pp. 1780–1787, Jul. 2014.
- [27] L. Wu and M. Shahidepour, "Optimal coordination of stochastic hydro and natural gas supplies in midterm operation of power systems," *Gener., Transmiss. Distrib.*, vol. 5, pp. 577–587, 2011.
- [28] C. Unsuhay *et al.*, "Short-term operation planning of integrated hydrothermal and natural gas systems," in *Proc. IEEE Power Eng. Soc. Gen. Meet.*, 2007, pp. 1410–1416.
- [29] B. C. Erdener *et al.*, "An integrated simulation model for analysing electricity and gas systems," *Int. J. Electr. Power Energy Syst.*, vol. 61, pp. 410–420, 2014.
- [30] C. Liu, M. Shahidepour, and J. Wang, "Coordinated scheduling of electricity and natural gas infrastructures with a transient model for natural gas flow," *Chaos, Interdisciplinary J. Nonlinear Sci.*, vol. 21, no. 2, 2011, Art. no. 025102.
- [31] M. Chaudry, N. Jenkins, and G. Strbac, "Multi-time period combined gas and electricity network optimisation," *Electric Power Syst. Res.*, vol. 78, no. 7, pp. 1265–1279, 2008.
- [32] H. Rachford and R. Carter, "Optimizing pipeline control in transient gas flow," *Pipeline Simulation Interest Group*, 2000.
- [33] M. Steinbach, "On PDE solution in transient optimization of gas networks," *J. Comput. Appl. Math.*, vol. 203, no. 2, pp. 345–361, 2007.
- [34] A. Zlotnik, S. Dyachenko, S. Backhaus, and M. Chertkov, "Model reduction and optimization of natural gas pipeline dynamics," presented at the ASME Dynamic Systems Control Conf., Columbus, OH, USA, 2015, Paper V003T39A002.
- [35] A. Zlotnik, M. Chertkov, and S. Backhaus, "Optimal control of transient flow in natural gas networks," in *Proc. IEEE 54th Conf. Decision Control*, 2015, pp. 4563–4570.
- [36] L. Biegler and V. Zavala, "Large-scale nonlinear programming using IPOPT: An integrating framework for enterprise-wide dynamic optimization," *Comput. Chem. Eng.*, vol. 33, no. 3, pp. 575–582, 2009.
- [37] Federal Energy Regulatory Commission (FERC) order #787 [Online]. Available: www.ferc.gov/CalendarFiles/20131115164637-RM13-17-000.pdf
- [38] M. Parvania and A. Scaglione, "Unit commitment with continuous-time generation and ramping trajectory models," *IEEE Trans. Power Syst.*, to be published.
- [39] M. Chaudry, J. Wu, and N. Jenkins, "A sequential monte carlo model of the combined gb gas and electricity network," *Energy Policy*, vol. 62, pp. 473–483, 2013.
- [40] B. Stott, J. L. Marinho, and O. Alsac, "Review of linear programming applied to power system rescheduling," in *Proc. Power Ind. Comput. Appl. Conf.*, May. 1979, pp. 142–154.
- [41] M. Vrakopoulou *et al.*, "Probabilistic guarantees for the N-1 security of systems with wind power generation," presented at the Int. Conf. Probabilistic Methods Applied Power Systems, Istanbul, Turkey, 2012.
- [42] A. Thorley and C. Tiley, "Unsteady and transient flow of compressible fluids in pipelines—A review of theoretical and some experimental studies," *Int. J. Heat Fluid Flow*, vol. 8, pp. 3–15, 1987.
- [43] Gas-Grid Network and Case Study [Online]. Available: <https://db.tt/yLQa2cDz>
- [44] S. Grundel, L. Jansen, N. Hornung, T. Clees, C. Tischendorf, and P. Benner, "Model order reduction of differential algebraic equations arising from the simulation of gas transport networks," in *Progress in Differential-Algebraic Equations*. Berlin, Germany: Springer, pp. 183–205, 2014.
- [45] J. Ruths, A. Zlotnik, and J.-S. Li, "Convergence of a pseudospectral method for optimal control of complex dynamical systems," in *Proc. IEEE 50th Conf. Decision Control*, 2011, pp. 5553–5558.
- [46] T. W. K. Mak, P. Van Hentenryck, A. Zlotnik, H. Hijazi, and R. Bent, "Efficient dynamic compressor optimization in natural gas transmission systems," presented at the American Control Conf., Chicago, IL, USA, 2016.
- [47] C. Grigg *et al.*, "The IEEE reliability test system-1996. A report prepared by the reliability test system task force of the application of probability methods subcommittee," *IEEE Trans. Power Syst.*, vol. 14, no. 3, pp. 1010–1020, Aug. 1999.
- [48] W. Katzenstein and J. Apt, "Air emissions due to wind and solar power," *Environ. Sci. Technol.*, vol. 43, no. 2, pp. 253–258, 2008.
- [49] R. D. Zimmermann *et al.*, "Matpower: Steady-state operations, planning, and analysis tools for power systems research and education," *IEEE Trans. Power Syst.*, vol. 26, no. 1, pp. 12–19, Feb. 2011.



Anatoly Zlotnik (M'11) received the B.Sc and M.Sc. degrees in systems and control engineering from Case Western Reserve University, Cleveland, OH, USA, both in 2006, the M.Sc. degree in applied mathematics from the University of Nebraska—Lincoln, Lincoln, NE, USA, in 2009, and the Ph.D. degree in systems science and mathematics from Washington University, St. Louis, MO, USA, in 2014. He is currently a Postdoctoral Research Associate at the Center for Nonlinear Studies and the Theoretical Division at Los Alamos National Laboratory, Los Alamos, NM,

USA.



Line Roald (M'12) received the B.Sc. and M.Sc. degrees in mechanical engineering from ETH Zürich, Zurich, Switzerland, in 2009 and 2012, respectively, where she is currently working toward the Ph.D. degree at the Power Systems Laboratory, Department of Electrical and Computer Engineering. Her research interests include modeling and optimization of power system operation under consideration of uncertainty and risk-based security criteria.

Scott Backhaus received the Ph.D. degree in physics from the University of California at Berkeley, Berkeley, CA, USA, in 1997, in the area of macroscopic quantum behavior of superfluid He-3 and He-4. He is currently the Principal Investigator for several LANL projects funded by the Office of Electricity in the U.S. Department of Energy, is an LANL Program Manager for Office of Electricity and for DHS Critical Infrastructure, and leads LANL's component of the DHS National Infrastructure Simulation and Analysis Group.



Michael Chertkov received the M.Sc. degree in physics from Novosibirsk State University, Novosibirsk, Russia, in 1990, and the Ph.D. degree in physics from the Weizmann Institute of Science, Rehovot, Israel, in 1996. For three years, he was with the Department of Physics, Princeton University, Princeton, NJ, USA, as an R. H. Dicke Fellow. He joined Los Alamos National Lab, Los Alamos, NM, USA, in 1999, first as a J. R. Oppenheimer Fellow in the Theoretical Division, and is currently a Technical Staff Member in the same division. He has published more than 150 papers in the areas of statistical and mathematical physics applied to energy and communication networks, machine learning, control theory, information theory, computer science, fluid mechanics, and optics. He is an Editor of the *Journal of Statistical Mechanics*, an Associate Editor of the IEEE TRANSACTIONS ON CONTROL OF NETWORK SYSTEMS, a Member of the Editorial Board of *Scientific Reports*, and a Fellow of the American Physical Society.



Göran Andersson (M'86–SM'91–F'97) received the M.S. and Ph.D. degrees from the University of Lund, Lund, Sweden, in 1975 and 1980, respectively. He joined ASEA in 1980, and in 1986, he became a full Professor in Electric Power Systems at the KTH Royal Institute of Technology, Stockholm, Sweden. Since 2000, he has been a full Professor in electric power systems at ETH Zürich, Zurich, Switzerland. His research includes include power systems dynamics and control, power markets, and future energy systems. He is a Fellow of the Royal Swedish Academy of Sciences, and of the Royal Swedish Academy of Engineering Sciences. He received the IEEE PES Outstanding Power Educator Award 2007 and the George Montefiore International Award 2010.